Photolysis of Matrix Isolated HONO/SO_2 System. Identification and Infrared Spectra of Nitrososulfonic Acid HO(NO)SO_2 and Hydroxysulfonyl $HOSO_2$ Radical

M. Wierzejewska* and A. Olbert-Majkut

Faculty of Chemistry, University of Wrocław, F. Joliot-Curie 14, 50383 Wrocław, Poland

Received: July 17, 2003; In Final Form: September 25, 2003

The HONO/SO_2/N_2 and HONO/SO_2/Ar matrixes were subjected to UV radiation ($\lambda > 340$ nm) from a medium pressure mercury lamp. The products of the photolysis were studied experimentally by means of FTIR spectroscopy and theoretically by the ab initio MP2 method. Two species are formed in nitrogen matrixes: the hydroxysulfonyl radical $HOSO_2$ and identified for the first time nitrososulfonic acid HO(NO)SO_2. In solid argon only, the latter species was observed. The identities of the products have been confirmed by carrying out experiments with deuterated nitrous acid DONO in place of HONO, performing concentration and annealing studies, comparison with results of quantum chemical calculations, and reference to the spectral data of related molecules. The mechanism of the photolytic reaction in the studied HONO/SO_2/N_2 and HONO/SO_2/Ar matrixes is discussed on the basis of the observed kinetic profiles of the precursor species and the products.

Introduction

Nitrous acid HONO is known as one of the most important sources of the OH radicals in the atmosphere[1] according to the dissociation channels:

$$\begin{aligned} \text{HONO } (+h\nu) &\rightarrow \text{OH}(X^2\Pi) + \text{NO}(X^2\Pi) \quad \Delta H_0{}^{\circ} = 48.0 \text{ kcal/mol} \\ &\rightarrow \text{OH}(A^2\Sigma) + \text{NO}(X^2\Pi) \quad \Delta H_0{}^{\circ} = 140.6 \text{ kcal/mol} \quad (1) \end{aligned}$$

In turn, hydroxyl radicals react in the atmosphere with a number of key species such as CO, SO_2, or organic compounds. The reaction of OH and SO_2 to form hydroxysulfonyl radical

$$\text{OH} + \text{SO}_2\ (+\text{M}) \rightarrow \text{HOSO}_2\ (+\text{M}) \quad (2)$$

is recognized to be the major rate-controlling step in the gas-phase oxidation of sulfur dioxide in the troposphere.[2] The $HOSO_2$ radical is further oxidized to H_2SO_4, although the mechanism is more complex than just the addition of a second OH radical.[3] Since early reports published by Cox[4] on photolysis of gaseous HONO/SO_2 system, many papers appeared on kinetics of reaction 2 using various experimental techniques.[5−10] The existence of the $HOSO_2$ radical has been proven in the gas phase by neutralization/reionization mass spectroscopy[11] and by FTIR spectroscopy in low-temperature matrixes.[12−14] The hydroxysulfonyl radical was also studied theoretically by Nagase et al.[13] Very recently, Aaltonen and Francisco[15] examined $HOSO_2$ and its complex with water using MP2 and B3LYP methods in the aim to investigate their possible role in the sulfuric acid production in the atmosphere.

It seemed interesting to study the HONO−SO_2 complex and its UV photolysis and to follow possible ways of the reaction between OH and NO radicals with sulfur dioxide. We present here a combined experimental (FTIR) and theoretical study of UV photolysis of the HONO/SO_2 system isolated in nitrogen and argon matrixes.

Experimental Section

The detailed description of the experimental setup has been given earlier.[16] Briefly, the HONO (and NH_3) was evaporated from a small glass bulb containing solid ammonium nitrite NH_4NO_2 maintained at 0 °C. The bulb was situated in the vacuum chamber of the cryostat at ca. 20 cm apart from the sample holder. The SO_2/N_2(Ar) gas mixtures were deposited through a separate inlet in such a way that they mixed with HONO(NH_3) vapors inside the vacuum vessel. For DONO experiments, the ND_4NO_2 was used as a nitrous acid source. The gas mixtures have been deposited onto a gold-coated copper mirror maintained typically at 15 or 18 K for nitrogen or argon depositions, respectively, by means of a closed cycle helium cryostat (Air Products, Displex 202A). Infrared spectra between 4000 and 500 cm^{-1} were recorded at 11.5 K in a reflection mode with a resolution of 0.5 cm^{-1} by means of a Bruker 113v FTIR spectrometer equipped with a liquid nitrogen cooled MCT detector.

The concentration of the HONO/N_2 or HONO/Ar matrixes is estimated to be 1/800−1/1000. The SO_2/N_2 and SO_2/Ar mixtures were prepared by standard manometric techniques, and their concentration was equal to 1/300, 1/600, and 1/3000. SO_2 (Matheson Gas Products) was purified by trap-to-trap distillation.

The matrixes were irradiated with a 200 W medium-pressure mercury lamp (Philipps CS200W2). A 10 cm thick water filter was placed between the lamp and the sample to reduce the infrared output of the arc. UV light was filtered by means of the glass long wavelength pass filter (Zeiss WG345) to cut off the radiation with $\lambda < 340$ nm.

Results

Matrix Isolation Studies. *Parent Molecules Spectra and Their Photolysis.* The infrared spectra of SO_2 and HONO isolated separately in nitrogen and argon matrixes have been

---

* To whom correspondence should be addressed. Fax: (48) 71 3282347. Phone: (48) 71 3757332. E-mail: mw@wchuwr.chem.uni.wroc.pl.

10.1021/jp036073x CCC: \$25.00

TABLE 1: Frequencies (cm^{-1}) and Frequency Shifts (cm^{-1})^a Observed for HONO−SO_2 Complexes Isolated in Nitrogen and Argon Matrixes

nitrogen matrix				argon matrix^b		
trans-HONO−SO_2	*cis*-HONO−SO_2	*trans*-DONO−SO_2	*cis*-DONO−SO_2	*trans*-HONO−SO_2	*cis*-HONO−SO_2	assignment
3479.8 (−71.7)	3352.2 (−54.7)	2570.4 (−51.6)	2474.2 (−44.6)?	3519.5 (−51.0)	3372.3 (−40.1)	ν_1 OH/ν_1 OD stretch
	3346.9 (−60.0)					
1676.8 (−4.3)	1625.5 (−4.8)	1661.8 (−11.1)		1673.8 (- 14.2)	1621.9 (−10.9)	ν_2 N═O stretch
	1623.9 (−6.4)	1660.9 (−12.0)				
831.3 (+16.6)	880.8 (+15.8)	790.6 (+22.6)	845.6 (+17.7)	814.1 (+17.5)		ν_4 N−O stretch
830.0 (+15.3)	879.6 (+14.6)		844.2 (+16.3)			
645.5 (+20.1)	670.8 (+11.5)			625.6 (+16.9)		ν_5 NO_2 bend
643.5 (+18.1)						
				1150.1 (−1.9)		ν_1 SO_2 sym. stretch
532.5 (+11.3)						ν_2 SO_2 bend

[a] Frequency shifts relative to the trans-HONO, cis- HONO and SO_2 monomers are given in parentheses. [b] Data from reference.[24]

TABLE 2: Observed and Calculated Frequencies (cm^{-1}) and Relative Intensities^a of $HOSO_2$ and $DOSO_2$ Radicals (Species A)

experiment			MP2 calculations			
nitrogen matrix		argon matrix^b	6-311++G(2df,2p)^c	6-311++G(3df,3pd)		
$HOSO_2$	$DOSO_2$	$HOSO_2$	$HOSO_2$	$HOSO_2$	$DOSO_2$	assignment
3475.7 (1.30)	2567.0 (1.34)	3539.9	3776 (0.52)	3789 (0.54)	2747 (0.25)	ν OH/ν OD
1311.7 (1.00)	1303.8 (1.00)	1309.2	1419 (1.00)	1427 (1.00)	1387 (1.00)	ν_{as} SO_2
		1296.2^d	1163 (0.38)	1174 (0.39)	865 (0.17)	δ SOH/δ SOD
1102.6 (0.61)	1103.6 (0.41)	1097.3	1131 (0.23)	1112 (0.27)	1135 (0.30)	ν_s SO_2
786.8 (0.79)	783.3 (0.73)	759.5	790 (0.62)	799 (0.63)	745 (0.48)	ν S−O
538.4 (0.15)	538.0 (0.31)		552 (0.11)	556 (0.11)	540 (0.10)	δ_{op} SO_2
			438 (0.11)	437 (0.15)	245 (0.14)	τ OH/τ OD
			435 (0.06)	436 (0.05)	422 (0.03)	δ_{ip} SO_2
			317 (0.27)	320 (0.28)		

[a] Relative intensities are given in parentheses. [b] Data from references.[12−14] [c] Data from reference.[15] [d] Reported only in ref 14.

TABLE 3: Observed and Calculated Frequencies (cm^{-1}) and Relative Intensities^a of HO(NO)SO_2 and DO(NO)SO_2 (Species B)

experiment^b				calculations MP2/6-311++G(3df,3pd)				
nitrogen matrix		argon matrix		HO(NO)SO_2		DO(NO)SO_2		
HO(NO)SO_2	DO(NO)SO_2	HO(NO)SO_2	DO(NO)SO_2	trans	cis	trans	cis	assignment
3510.2 sh	2591.7 sh	3551.5	2622.0	3795 (0.71)	3794 (0.67)	2762 (0.42)	2761 (0.40)	ν OH/ν OD
3502.2 (0.48)	*2585.6* (0.37)	*3548.8* (0.81)	*2620.2* (0.75)					
1650.8 (0.72)	1650.8^c	1646.6 sh	1644.8^c	1595 (1.07)	1590 (1.07)	1594 (1.09)	1590 (1.09)	ν NO
		1644.3 (0.81)	1643.7					
1401.5 (1.00)	*1397.2* (1.00)	1410.7	1406.9	1464 (1.00)	1463 (1.00)	1459 (1.00)	1458 (1.00)	ν_{as} SO_2
1400.5	1395.5	*1409.6* (1.00)	*1405.7* (1.00)					
	1394.8							
1184.6 (0.28)	*1182.1* (0.46)	1186.2	1185.3	1220 (0.71)	1221 (0.71)	1221 (0.70)	1221 (0.67)	ν_s SO_2
1183.4 sh	1180.2	*1184.4* (0.27)	*1184.1* (0.51)					
1175.2 (0.41)				1116 (0.32)	1114 (0.29)	860 (0.77)	852 (0.85)	δ SOH/δ SOD
1173.8								
849.7	*846.6*^{c}	834.7 (0.31)	831.8 (0.19)	848 (0.99)	844 (1.02)	836 (0.39)	837 (0.35)	ν S−O
844.1 (0.96)	837.5	829.0	825.7					
841.6 sh								
				675 (0.15)	674 (0.07)	670(0.13)	670 (0.08)	ν S−N
590.2 (0.19)	587.7 (0.08)	586.1 (0.14)	584.5 (0.20)	596 (0.22)	595 (0.19)	592 (0.24)	595 (0.21)	δ_{op} SO_2
	586.7							
				467 (0.10)	465 (0.12)	464 (0.09	461 (0.10)	δ_{ip} SO_2
				436 (0.09)	442 (0.21)	401 (0.05)	401 (0.11)	τ OH/τ OD

[a] Relative intensities are given in parentheses. [b] Component with higher intensity is italicized. [c] The relative intensity not estimated due to the band overlapping.

recorded and are in close agreement with those previously published.[16−21] The results of the UV photolysis of nitrous acid and sulfur dioxide in low-temperature matrixes have been also reported earlier.[22,23] At the conditions of the present experiment (λ > 340 nm), HONO was found to dissociate exclusively into OH and NO radicals, whereas the SO_2 molecule is photostable until 220 nm.

Nitrous Acid Complex with Sulfur Dioxide Isolated in Nitrogen and Argon Matrixes. The infrared spectra of the *trans*-HONO−SO_2 and *cis*-HONO−SO_2 1:1 complexes isolated in argon matrixes and ab initio calculations for these systems have been already reported.[24] Because the results obtained for nitrogen matrixes are in general agreement with those found for solid argon, they will be only briefly discussed. Deposition of the HONO/SO_2/N_2 mixtures gave rise to several new features situated in the vicinity of both HONO-trans and HONO-cis modes. The wavenumbers of these absorptions are gathered in Table 1 together with those found in argon matrixes. The shifts relative to the corresponding monomer vibrations are given in parentheses. The relative intensities of these bands are constant in the studied range of concentrations indicating that all belong to the 1:1 species. At the SO_2 concentration used in the present

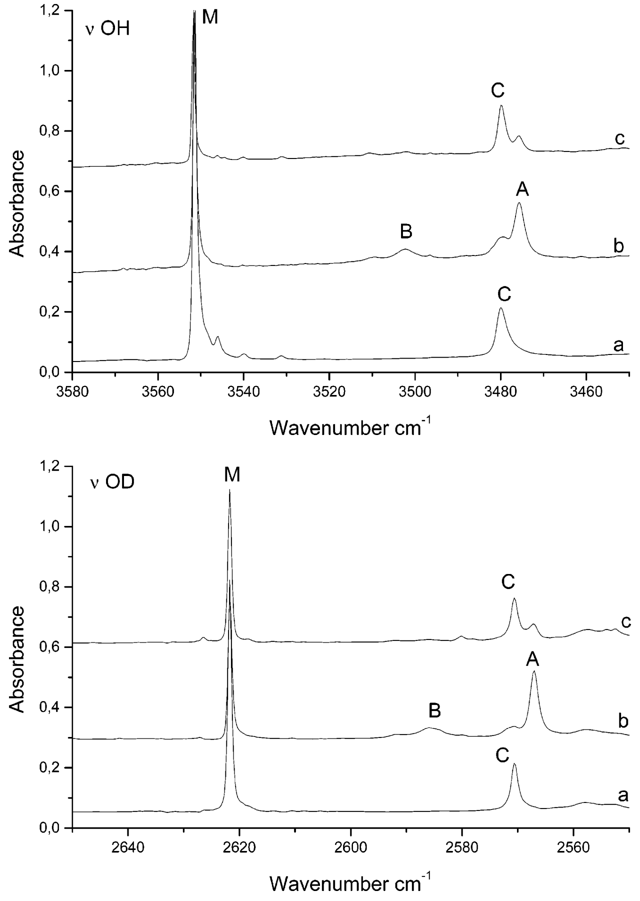

Figure 1. FTIR spectra of HONO/SO_2/N_2 (upper) and DONO/SO_2/N_2 (lower) matrixes of composition ca. 1/1.5/900 in the 3580−3450 and 2650−2550 cm^{-1} regions: (a) spectrum recorded directly after deposition, (b) spectrum a after 120 min of photolysis at $\lambda > 340$ nm, (c) spectrum b after 10 min annealing at 28 K and recooling to 11.5 K. A, B, C, and M denote product A, product B, HONO−SO_2 complex, and HONO monomer, respectively.

experiment, no absorptions due to higher aggregates of HONO−$(SO_2)_n$ have been detected. On the basis of the observed frequency shifts, the same as that in the argon type of the structure may be concluded for the *trans*-HONO−SO_2 and *cis*-HONO−SO_2 complexes isolated in nitrogen, with OH group interacting with one of the oxygen atoms of sulfur dioxide molecule.

Photolysis of HONO/SO_2/N_2 Matrixes. In the spectra recorded directly after matrix deposition, the absorptions due to *trans*- and *cis*-HONO isomers, SO_2 monomers and dimers, and *trans*-HONO−SO_2 and *cis*-HONO−SO_2 complexes were identified. Photolysis of the deposited precursor HONO/SO_2/N_2 matrixes using filtered radiation ($\lambda > 340$ nm) from a medium-pressure mercury lamp have created new species as was evident by the emergence of new bands. The positions of absorptions which appeared on photolysis of HONO/SO_2/N_2 samples independently on the concentration used are given in the first columns of Tables 2 and 3. Spectral regions of particular interest are shown in Figures 1−5.

On irradiation, the following changes are observed in the spectra of HONO/SO_2/N_2 matrixes:

(1) Depletion with different ratios of the HONO−SO_2, HONO bands as presented in Figure 6 for ν_4 N−O band (830.0 cm^{-1}) of trans-HONO−SO_2 complex, ν_4 N−O band (814.7 cm^{-1}) of trans-HONO and a slight decrease of sulfur dioxide absorptions as shown for ν_2 SO_2 band (521.2 cm^{-1}) (curves 1, 2 and 3, respectively).

(2) A set of bands appears at 3475.7, 1311.7, 1102.6, 786.8, and 538.4 cm^{-1} (see Table 2) and proceeds to grow in the same manner with the photolysis time increase according to the curves 4 (1311.7 cm^{-1}) and 5 (786.8 cm^{-1}) in Figure 6. We name the species corresponding to this set of absorptions as A for now.

(3) There is a second set of bands growing, most of them appearing as doublets or triplets at 3510.2/3502.2, 1650.8, 1401.5/1400.5, 1184.6/1183.4sh, 1175.2/1173.8, 849.7/844.1/841.6, and 590.2 cm^{-1} (see Table 3). We name the species corresponding to these absorptions as B. The intensities of these absorptions change differently than those attributed to the species A. It is also presented in Figure 6 as traces 6 (1650.8 cm^{-1}) and 7 (1401.5/1400.5 cm^{-1}).

(4) When deuterated nitrous acid DONO is used in place of HONO, new product bands are observed which may be also divided into two sets of absorptions corresponding to species A and B. The positions of these absorptions are gathered in the second columns of Tables 2 and 3.

The relative intensities of the bands assigned to either A or B product were constant within experimental error in all studied spectra.

Photolysis of HONO/SO_2/Ar Matrixes. Photolysis of the deposited precursor HONO/SO_2/Ar matrixes at the same irradiation conditions as applied for nitrogen matrixes leads to the appearance of only one set of bands situated close to the absorptions found for species B in solid N_2. Upon deuteration of the precursor matrixes, new product bands grow on photolysis in the corresponding spectral regions. All new frequencies appearing in the HONO/SO_2/Ar and DONO/SO_2/Ar spectra are gathered in third and forth columns of Table 3, and the ν OH and ν OD regions of the spectra are presented in Figure 7.

Bands due to the species A do not show up in the studied spectra indicating that only one new product appears after photolysis in solid argon.

Annealing of the Photolyzed HONO/SO_2/N_2 and HONO/SO_2/Ar Matrixes. On annealing of the photolyzed HONO/SO_2/N_2 and HONO/SO_2/Ar matrixes, the following changes are observed in the spectra:

(1) Additional weak bands grow up on annealing in the vicinity of A and B product absorptions (in N_2 matrix) or close to product B absorptions (Ar matrix). Positions of these features are gathered in Table 4 together with their shifts relative to the corresponding A or B bands.

(2) Product band intensities decrease,

(3) The *trans*-HONO−SO_2 complex is partly reproduced in the matrix as evidenced by growth of the corresponding absorptions as presented for ν OH and ν OD regions in Figures 1 and 7 (traces c).

Computational Details and Results

All calculations were performed within the framework of the ab initio approach using the Gaussian 98 package of computer codes.[25] The following species have been considered: HO(NO)SO_2, HO(NO)SO_2−SO_2, $HOSO_2$, and $HOSO_2$−SO_2. A second-order Möller−Plesset perturbation theory (MP2) was applied for two former species, whereas the unrestricted Möller−Plesset theory (UMP2) was used for the two latter compounds.[26,27]

Structures of the $HOSO_2$ and HO(NO)SO_2 species were fully optimized using both 6-311++G(2d,2p) and 6-311++G(3df,3pd) basis sets, whereas for their complexes with SO_2 only, the 6-311++G(2d,2p) basis set was chosen. For nitrososulfonic acid HO(NO)SO_2, two stable isomers were found corresponding to the trans and cis conformations. The structures of these isomers

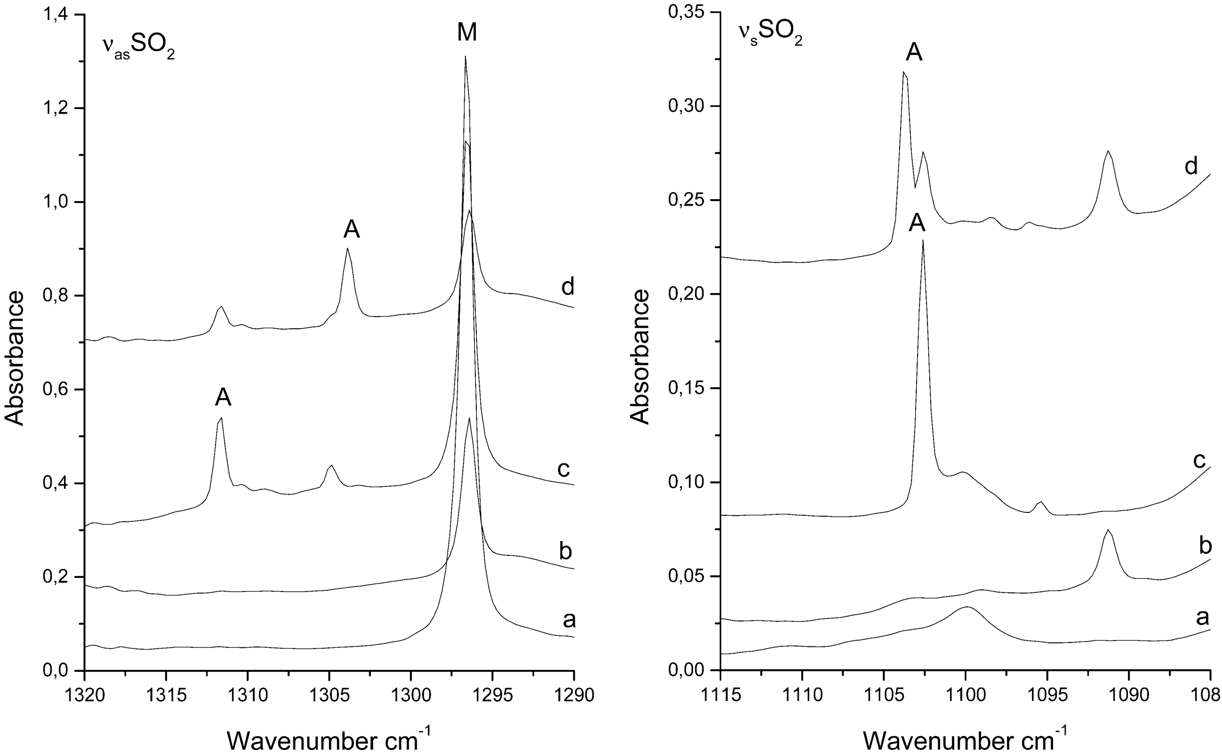

Figure 2. FTIR spectra of HONO/SO$_2$/N$_2$ (a and c) and DONO/SO$_2$/N$_2$ (b and d) matrixes of composition ca. 1/3/900 in the 1320−1290 and 1115−1085 cm^{-1} regions: (a and b) spectra recorded directly after deposition; (c and d) spectra a and b after 120 min ofphotolysis at $\lambda > 340$ nm. A denotes product A.

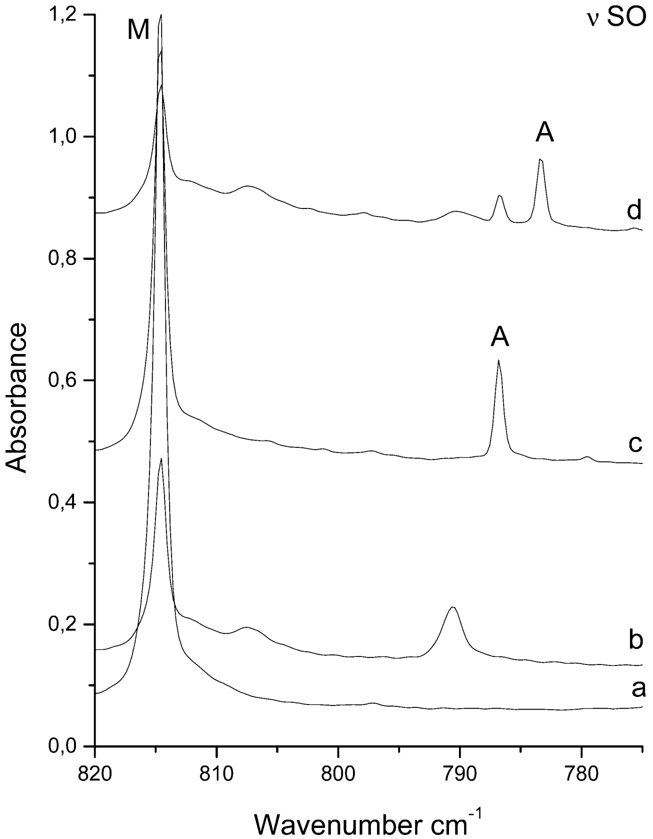

Figure 3. FTIR spectra of HONO/SO$_2$/N$_2$ (a and c) and DONO/SO$_2$/N$_2$ (b and d) matrixes of composition ca. 1/3/900 in the 820−770 cm^{-1} region: (a and b) spectra recorded directly after deposition; (c and d) spectra a and b after 120 min of photolysis at $\lambda > 340$ nm. A denotes product A.

differ in the orientation of the NO and OH units in the molecule. The optimized geometrical parameters of the two HO(NO)SO$_2$ conformers are presented in Table 5. Structural details for other species considered are not provided here but may be obtained from the Supporting Information (Table 1S). The optimized structures of all calculated species are presented in Figure 8.

Vibrational frequencies and intensities computed for HOSO$_2$, HO(NO)SO$_2$, and their complexes are reported in Tables 2, 3, and 2S, whereas energetics associated with the considered species is gathered in Table 3S. Interaction energies of complexes were corrected by the Boys−Bernardi full counterpoise correction at the MP2 or UMP2 level. Zero-point energies were calculated from the harmonic frequencies.

Until now, only the hydroxysulfonyl radical has been a subject of theoretical studies.[13,15] Both geometrical parameters and vibrational frequencies obtained here for HOSO$_2$ are in accord with those reported recently by Aaltonen and Francisco.[15]

Discussion

Identification of the Products. The results of the sulfur dioxide and nitrous acid photolysis in low-temperature matrixes have been already reported.[22,23] At the present conditions of the photolysis ($\lambda > 340$ nm), nitrous acid dissociation proceeds exclusively through the reaction HONO $\rightarrow$ OH + NO. The obvious candidate for one of the observed products (product A) is thus the *hydroxysulfonyl* radical HOSO$_2$. Three papers have been published so far dealing with matrix isolated HOSO$_2$ and its ab initio calculations.[12−15] The infrared spectrum of HOSO$_2$ in solid argon is relatively well-known; however, there is no data available on nitrogen matrixes. Both experimental and theoretical results on HOSO$_2$ are gathered in Table 2 together with our results obtained for species A in the spectra of the irradiated HONO/SO$_2$/N$_2$ and DONO/SO$_2$/N$_2$ matrixes. A comparison of the band positions of species A observed in the present study and those found for HOSO$_2$ in argon matrixes[12−14] confirms such an assignment for species A. The

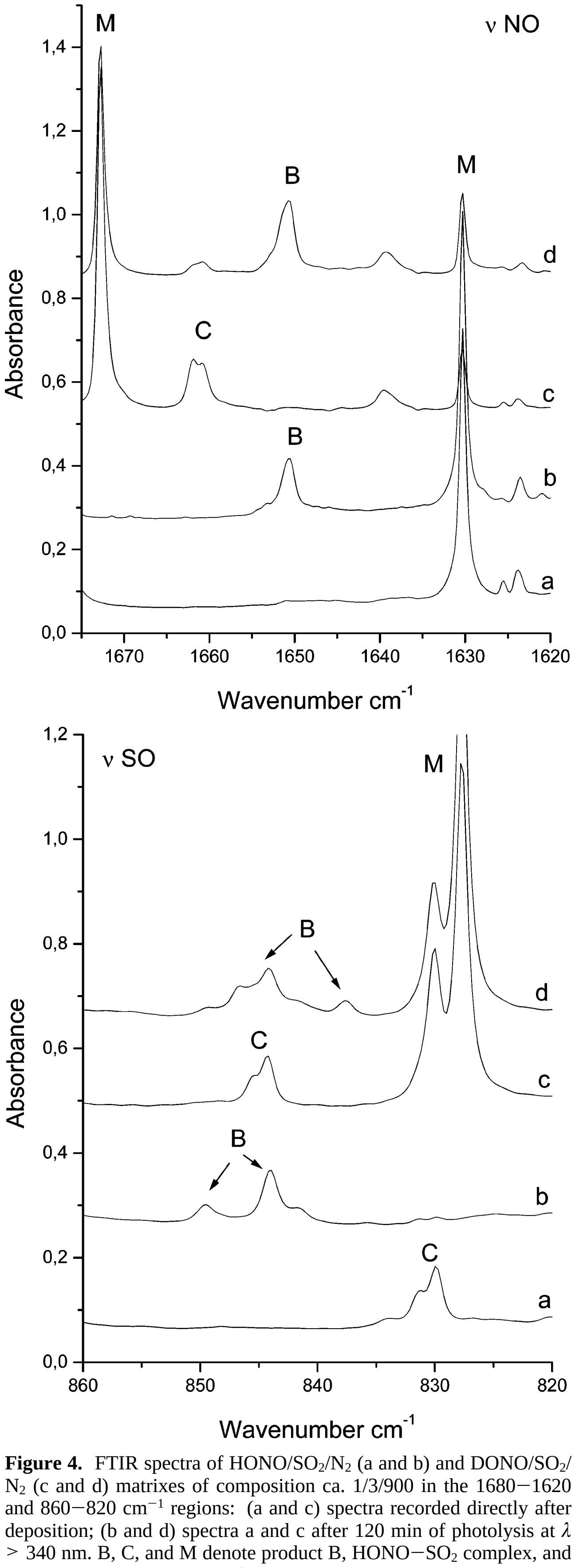

Figure 4. FTIR spectra of HONO/SO_2/N_2 (a and b) and DONO/SO_2/N_2 (c and d) matrixes of composition ca. 1/3/900 in the 1680−1620 and 860−820 cm^{-1} regions: (a and c) spectra recorded directly after deposition; (b and d) spectra a and c after 120 min of photolysis at $\lambda > 340$ nm. B, C, and M denote product B, HONO−SO_2 complex, and HONO monomer, respectively.

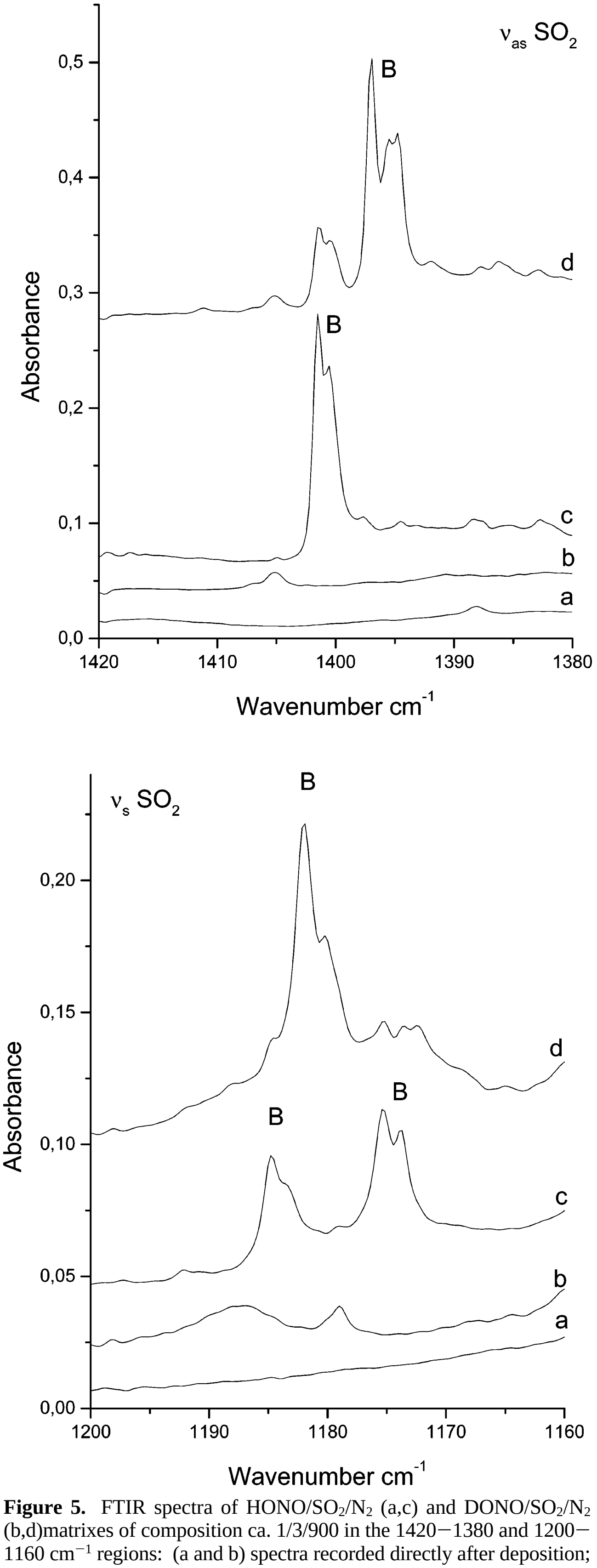

Figure 5. FTIR spectra of HONO/SO_2/N_2 (a,c) and DONO/SO_2/N_2 (b,d)matrixes of composition ca. 1/3/900 in the 1420−1380 and 1200−1160 cm^{-1} regions: (a and b) spectra recorded directly after deposition; (c and d) spectra a and b after 120 min of photolysis at $\lambda > 340$ nm. B denotes product B.

H/D ratio observed for 3475.7/2567.0 absorptions is equal to 1.35 and proves the presence of a hydroxyl group in the product A. Shifts on deuteration of other modes are also consistent with such an interpretation. The δ SOH deformation mode is not localized in our spectra. This absorption was found as a very weak absorption at 1296.2 cm^{-1} by Kuo et al.,[14] whereas it was not reported in two other papers.[12,13]

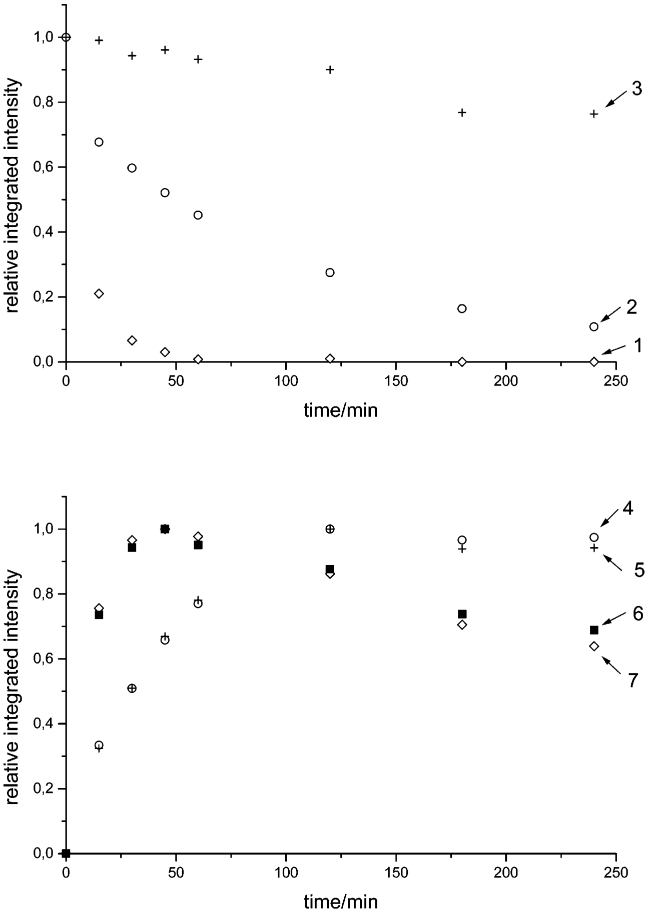

Figure 6. Plot of the relative integrated intensities versus time of the photolysis: **1** ν_4 N−O band (830.0 cm^{-1}) of *the* trans-HONO−SO$_2$ complex, **2** ν_4 N−O band (814.7 cm^{-1}) of the *trans*-HONO, **3** ν_2 SO$_2$ band (521.2 cm^{-1}) of sulfur dioxide monomer, **4**, **5** absorptions at 1311.7 and 786.8 cm^{-1} of product A (HOSO$_2$) **6**, **7** absorptions at 1650.8 and 1401.5/1400.5 cm^{-1} of product B.

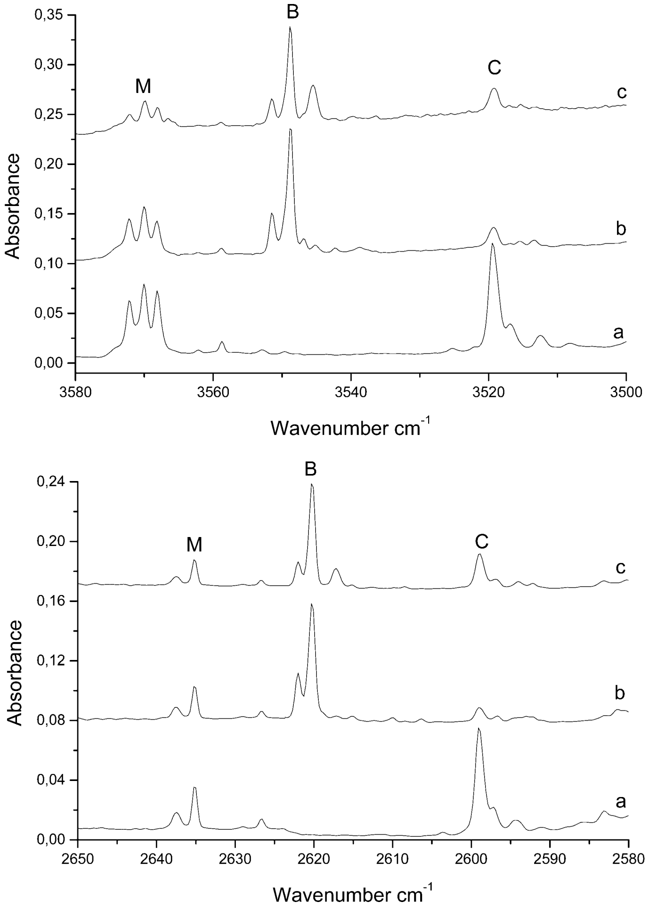

Figure 7. FTIR spectra of HONO/SO$_2$/Ar (upper) and DONO/SO$_2$/Ar (lower) matrixes of composition ca. 1/3/900 in the 3580−3500 and 2650−2580 cm^{-1} regions: (a) spectrum recorded directly after deposition, (b) spectrum a after 120 min of photolysis at λ > 340 nm, (c) spectrum b after 10 min annealing at 28 K and recooling to 11.5 K. B, C, and M denote product B, HONO−SO$_2$ complex, and HONO monomer, respectively.

A second set of bands appearing on photolysis of the HONO/SO$_2$/N$_2$ matrixes (species B) is attributed to the unobserved so far *nitrososulfonic acid* molecule HO(NO)SO$_2$. This assignment may be justified by the following arguments. Weak absorption at 3502.2/3510.2 cm^{-1} is situated in the range suitable for the OH stretching mode. Its counterpart in the isotopic experiment occurs at 2585.6/2591.7 cm^{-1} showing H/D ratio equal to ca. 1.36 as expected for this type of vibration. The presence of the nitroso unit in species B is confirmed by the appearance of the absorbance at 1650.8 cm^{-1} attributed to the NO stretching mode. This band is situated between of the ν_2 NO stretching modes of the trans (1681.3 cm^{-1}) and cis (1630.2 cm^{-1}) HONO monomers isolated in the N$_2$ matrix indicating the double bond character of the NO unit attached by the N end to the sulfur atom in the HO(NO)SO$_2$ molecule. Many examples of the species containing the NO nitroso group can be found in the literature. Some of them are gathered in Table 6. For example, Müller et al.[28] have studied thionitrous acid HSNO in low-temperature matrixes and have found the ν NO bands at 1596.0 and 1570.0 cm^{-1} for *trans*- and *cis*-HSNO isomers in solid argon. Lower position of this mode was reported very recently for two OSNO isomers isolated in nitrogen matrix at 1459.0 and 1454.4 cm^{-1}.[29] In turn, two NO stretches were localized at 1669.2 and 1567.3 cm^{-1} in the spectra of ONSNO.[30]

There is no noticeable shift on deuteration observed in our spectra for the ν NO mode; however, the intensity of this band in the spectra containing both HO(NO)SO$_2$ and DO(NO)SO$_2$ is much higher than that expected for the former product only. Tchir and Spratley[31] reported very small shifts of 2 cm^{-1} on deuteration for *trans*- and *cis*-HSNO molecules, and in the case of nitrososulfonic acid, an even smaller change may be expected because the NO unit is separated from the hydrogen/deuterium atom by one bond more in HO(NO)SO$_2$ than in HSNO. As can be seen in Table 3, our calculations have also predicted a negligible shift upon deuteration for the ν NO mode (1 cm^{-1}).

Three other absorptions belonging to the B product in the studied nitrogen matrix appear at positions consistent with the asymmetric (1401.5, 1400.5 cm^{-1}), symmetric (1184.6, 1183.4 cm^{-1}) stretching and bending (590.2 cm^{-1}) modes of the SO$_2$ subunit. The corresponding modes of the SO$_2$ monomer are situated at 1351.6, 1152.6, and 521.3 cm^{-1}.[18]

Two other modes of HO(NO)SO$_2$ are also localized in the studied spectra, namely, the SOH bending and S−O stretching situated at 1175.2, 1173.8 (doublet) and at 849.7, 844.1, 841.6 cm^{-1} (triplet), respectively. Their positions are comparable with those reported for sulfuric acid isolated in argon matrix at 1135.9 and 831.4 cm^{-1}.[32] For sulfinic HSOOH[33] and sulfenic HSOH[34] acids, the SOH bending and S−O stretching are reported at 1093, 762 and 1177, 763 cm^{-1}, respectively. We consider the assignment of the SOH bending mode as tentative because a δ SOD counterpart was not localized in the spectra. The S−N stretch escaped detection; however, our ab initio calculations predict its intensity to be extremely low (see Tables 3 and 2S).

TABLE 4: Frequencies (cm^{-1}) and Frequency Shifts (cm^{-1})of Bands Appearing upon Annealing in the Spectra of the Photolyzed $HONO/SO_2/N_2(Ar)$ Matrixes[a]

nitrogen matrix		argon matrix		MP2/6-311++G(2d,2p)[b]				
				A-SO_2,	*trans*-B−SO_2	*cis*-B−SO_2		
ν	$\Delta\nu$	ν	$\Delta\nu$	$\Delta\nu$	$\Delta\nu$	$\Delta\nu$	tentative assignment	species[a]
3243.1	−232.6			−185			ν OH	A-SO_2
1319.5	+7.8			−13			ν_{as} SO_2	A-SO_2
1101.7	−0.9			−5			ν_s SO_2	A-SO_2
801.2	+14.4			+32			ν S−O	A-SO_2
		3545.5	−3.3					B, site?
3281.3	−220.9				−186	−171		B−SO_2
1639.0	−11.8	1649.1	+4.8		−19	−15	ν NO	B−SO_2
1402.2	+0.7	1404.0	−5.6		−7	−10	ν_{as} SO_2	B−SO_2
1180.7	−3.9	1175.8	−8.6		−8	−11	ν_s SO_2	B−SO_2

[a] A comparison of the experimental and calculated data. [b] A and B denote $HOSO_2$ and $HO(NO)SO_2$, respectively.

TABLE 5: Calculated Geometry[a] of the *trans*- and *cis*-$HO(NO)SO_2$ Molecules

	$HO(NO)SO_2$			
	trans		cis	
parameter	(2d,2p)	(3df,3pd)	(2d,2p)	(3df,3pd)
r(H−O)	0.967	0.968	0.968	0.968
r(O−S)	1.631	1.592	1.633	1.594
r(S=O_1)	1.449	1.432	1.450	1.432
r(S=O_2)	1.442	1.424	1.443	1.424
r(S−N)	2.084	1.918	2.091	1.921
r(N=O)	1.163	1.180	1.164	1.181
θ(HOS)	106.6	108.3	106.5	108.0
θ(OSO_1)	107.5	108.9	107.5	109.2
θ(OSO_2)	106.3	107.1	106.3	106.8
θ(O_1SO_2)	124.2	124.8	124.2	124.8
θ($HOSO_1$)	−17.8	−20.5	14.5	15.9
θ($HOSO_2$)	−152.9	−157.9	153.3	153.4
θ(HOSN)	97.9	89.2	−96.3	−97.5
θ(OSNO)	112.5	118.5	113.9	118.2

[a] Bond lengths are in Å, and angles are in degrees.

In contrast to the bands assigned to the $HOSO_2$ radical, most of the absorptions attributed to the nitrososulfonic acid are present as doublets or triplets typically separated by few wavenumbers. Two explanations may be considered. The first one is the possibility of different trapping sites available for the $HO(NO)SO_2$ species in nitrogen matrixes. The second explanation comes from the results of ab initio calculations. Two isomers cis and trans are predicted to be stable for the nitrososulfonic molecule. Their energy calculated at the MP2/6-311++G(3df,3pd) level differs by 0.63 kcal/mol (0.69 kcal/mol using 6-311++G(2d,2p) basis set) with the trans isomer being more stable. So, a coexistence of both isomers in the studied matrixes would be justified. Frequencies calculated for cis and trans $HO(NO)SO_2$ differ by 1−4 cm^{-1} with the only exception found for the ν NO stretching mode where the difference is equal to 13 cm^{-1}. In turn, in the experimental spectra the ν NO mode is the only one that appears as a singlet (see Table 3).

As can be seen from Table 3, a set of bands observed on photolysis of $HONO/SO_2/Ar$ and $DONO/SO_2/Ar$ matrixes corresponds well to those assigned to nitrososulfonic acid in nitrogen matrixes, and thus, the only photoproduct formed in solid argon must be $HO(NO)SO_2$ and its deuterated analogue $DO(NO)SO_2$.

Annealing of the Photolyzed Matrixes. As mentioned earlier, in both nitrogen and argon matrixes, several processes proceed after matrix annealing. Because of the complexity of the system, the interpretation of the changes is not straightforward. The concentration of photoproducts decreases and new absorptions grow in the vicinity of the photoproducts bands. Because of the large quantity of SO_2 monomers present in the matrix, they may react with both $HOSO_2$ and $HO(NO)SO_2$ upon annealing. Our calculations have shown (Table 3S) that $HOSO_2-SO_2$, *trans*-$HO(NO)SO_2-SO_2$, and *cis*-$HO(NO)SO_2-SO_2$ complexes are stable with the interaction energies equal to 7.47, 8.09, and 8.91 kcal/mol, respectively. The frequencies calculated for these complexes are presented in Table 2S. The calculated frequency shifts for $HOSO_2-SO_2$ and both $HO(NO)SO_2-SO_2$ complexes are compared in Table 4 with those observed for new bands which grow on annealing in the vicinity of absorptions of both photoproducts. The shifts observed for ν OH and ν NO modes in $HOSO_2-SO_2$ and $HO(NO)SO_2-SO_2$ complexes in the nitrogen matrix are in accord with those calculated, whereas the agreement is worse for other modes and for argon matrix. Thus, we consider the

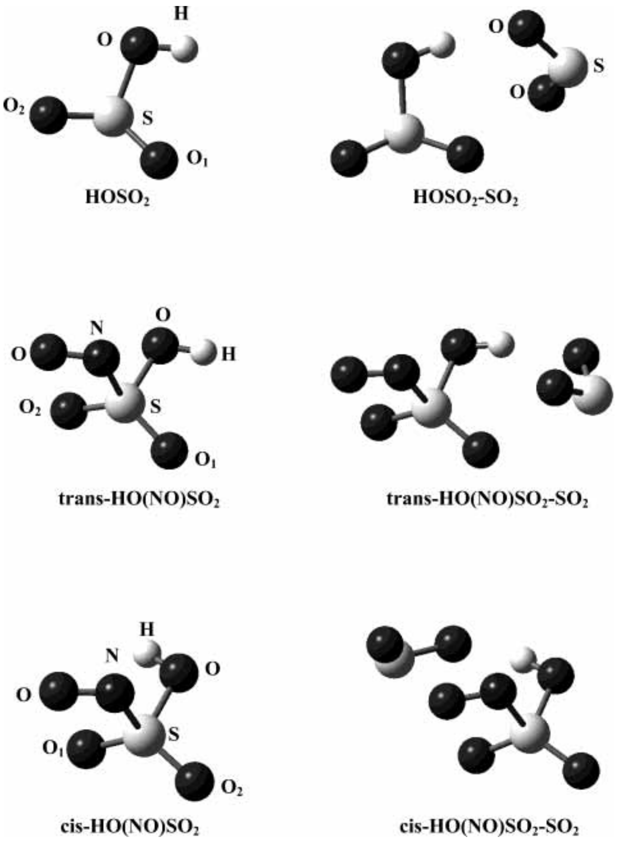

Figure 8. Optimized structures of the $HOSO_2$, $HOSO_2-SO_2$, *trans*-$HO(NO)SO_2$, *trans*-$HO(NO)SO_2-SO_2$, *cis*-$HO(NO)SO_2$, and *cis*-$HO(NO)SO_2-SO_2$ species at the MP2/6−311++G(2d,2p) level.

TABLE 6: Frequencies (cm^{-1}) of the NO Stretching Modes in Various Complexes and Small Molecules Containing an NO Unit Isolated in Argon and Nitrogen Matrixes

species	nitrogen matrix	argon matrix	ref
H_2SO_4−NO		1890	38
HNO_3−NO		1889	39
HF−NO		1887	40
HONO−NO	1882.0	1884.2, 1883.2	41
HCl−NO		1880	42
NO	1874.8	1871.8	22, 36
ClNO	1830.8	1805.9	43
BrNO	1822.8	1800.3, 1797.9	43
PNO		1754.7	44
HOONO	1701.4	1703.6	45
ONNC		1681.0	46
ONSNO		1669.2, 1567.3	30
HO(NO)SO_2	1650.8	1644.3	this work
cis-HONO; *trans*-HONO	1630.2, 1681.3	1688.2, 1632.8	16
cis-HSNO; *trans*-HSNO		1570.0; 1596.0	28, 31
HNO	1568.5	1563.2	47
SNO		1522.8	30, 48
ONCN		1498.5	46
cis-OSNO, *trans*-OSNO	1454.4; 1459.0	1450.8; 1456.0	29

assignment presented in Table 4 as tentative. Further studies would be needed for the precise assignment of the observed features.

Another process which is observed upon annealing, namely, reproduction of the initial HONO−SO_2 or DONO−SO_2 complex, may be due to the recombination of OH and NO radicals (those which escaped reaction during photolysis) with SO_2 trapped in the same or neighboring cage.

Photochemical Pathway. The analysis of the kinetic profiles presented in Figure 6 shows that HO(NO)SO_2 is produced in nitrogen matrixes relatively quickly, reaches a maximum concentration, and is then removed by further photolysis (traces 6 and 7). The turning point on curves 6 and 7 coincides with the region when the HONO−SO_2 complex bands decline (Figure 6, trace 1). These results suggest that nitrososulfonic acid is produced exclusively from the HONO−SO_2 complex.

The product A, the $HOSO_2$ radical (traces 4 and 5), shows the inflection point in its growth curves which is an indication of a consecutive reaction. Because the inflection point on the $HOSO_2$ curve falls near the maximum in the HO(NO)SO_2 concentration, most probably, the hydroxysulfonyl radical is produced to a great extent from HO(NO)SO_2 molecules. Because the lowest dissociation energy of nitrous acid proceeding via the HONO → $OH(X^2\Pi) + NO(X^2\Pi)$ channel is equal to 48.0 kcal/mol[35] the radiation of the wavelength with $\lambda >$ 340 nm ($E <$ 84 kcal/mol) used in the present experiment produces OH and NO radicals with some excess of energy. In turn, photodissociation of the HONO−SO_2 complex leads to the hot OH and NO radicals trapped together with the SO_2 molecule in the same matrix cage. The radicals may further react to form nitrososulfonic acid. A part of the HO(NO)SO_2 molecules will be stabilized in the matrix cage, whereas others with sufficient energy or as a result of further photolysis will dissociate to form $HOSO_2$ and NO radicals. The latter species may escape from the cage leaving $HOSO_2$ radicals in there. According to our ab initio calculations, the NO radical is relatively weakly bonded to the sulfur atom in nitrososulfonic acid as evidenced by a rather high value obtained for the N−S bond distance equal to 1.92 Å (at MP2/6-311++G(3df,3pd)).

As can be seen in Figure 6 (trace 3), a slight decrease of the SO_2 monomer bands on irradiation is observed in the spectra of HONO/SO_2/N_2 matrixes. This suggests that some of the $HOSO_2$ radicals are produced as a result of the reaction of OH radicals with sulfur dioxide molecules. According to the latest studies, the $SO_2 + OH \rightarrow HOSO_2$ reaction proceeds either without energy barrier[10] or with a small one of ca. 0.72 kcal/mol[9] which would be easy overcome at the condition of the experiment.

The fact that only nitrososulfonic acid is produced in argon matrixes containing HONO/SO_2 deserves some comment. In contrast to the situation in solid nitrogen, we do not observe the ν NO stretch of the free radical in the spectra of the irradiated HONO/SO_2/Ar matrixes, expected at 1871.8 cm^{-1}.[36] This confirms a very limited cage exit of NO radicals in argon, whereas in nitrogen, NO diffuses much easier. It was suggested that due to the very similar bond lengths of NO and N_2 the direct interchange between these molecules in the nitrogen matrix and thus the diffusion process may be relatively easy.[37] If it is so, the formation of not only HO(NO)SO_2 but also $HOSO_2$ in solid nitrogen would be justified, whereas in argon matrixes, exclusively nitrososulfonic acid HO(NO)SO_2 should be formed. Further photolysis may cause the cleavage of the S−N bond; however, unlike the situation in solid nitrogen the recombination occurs before NO radical escapes the cage. Diffusion of the OH radicals formed from the HONO monomer photolytic reaction at the condition of the experiment must not be of importance in solid argon because there is no evidence for the second channel of the hydroxysulfonyl radical production: $SO_2 + OH \rightarrow HOSO_2$.

These considerations do not contradict the results of earlier work on $HOSO_2$ isolated in solid argon.[12−14] In all previous cases, the $HOSO_2$ species were formed in the gas phase during deposition and not as a result of OH radicals diffusion in the matrix.

Summary

It was shown by means of FTIR spectroscopy that the UV photolysis ($\lambda >$ 340 nm) of HONO/SO_2/N_2 matrixes led to the formation of two products: the hydroxysulfonyl radical $HOSO_2$ and, identified for the first time, nitrososulfonic acid HO(NO)SO_2. The results of quantum chemical calculations confirmed the identities of these two products. The obtained kinetic profiles revealed that nitrososulfonic acid HO(NO)SO_2 is formed exclusively from the HONO−SO_2 complex. The hydroxysulfonyl radical is produced to a great extent from HO(NO)SO_2; however, the second channel is also present and a part of $HOSO_2$ radicals is formed as a result of the reaction of OH radicals with sulfur dioxide molecules.

The photolysis of HONO−SO_2 complexes isolated in argon matrixes produced only one product: nitrososulfonic acid. This observation confirmed a rather limited cage exit of NO radicals and a negligible diffusion of OH radicals at the present experimental conditions in solid argon.

Acknowledgment. We thank Prof. Zofia Mielke for stimulating discussions and prof. Konstantin Tokhadze for his help during the photolysis setup arrangement. We gratefully acknowledge a grant of computer time from the Wrocław Center for Networking and Supercomputing.

Supporting Information Available: Calculated geometries and infrared spectra for $HOSO_2$, $HOSO_2$−SO_2, HO(NO)SO_2, HO(NO)SO_2−SO_2 species at the MP2 level. Calculated (MP2/6-311++G(2d,2p)) energies for $HOSO_2$, HO(NO)SO_2, and their complexes with SO_2. This material is available free of charge via the Internet at http://pubs.acs.org.

References and Notes

(1) Finlayson-Pitts, B. J.; Pitts, J. N., Jr. *Atmospheric Chemistry*: *Fundamentals and Experimental Techniques*; Wiley&Sons: New York, 1985.

(2) Stockwell, W. R.; Calvert, J. G. *Atmos. Environ*. **1983**, *17*, 2231.

(3) Wayne, R. P. *Chemistry of Atmospheres*; Clarendon Press: Oxford, 1991.

(4) Cox, R. A. *J. Photochem.* **1974/75**, *3*, 291.

(5) Wine, P. H.; Thompson, R. J.; Ravishanakara, A. R.; Semmes, D. H.; Gump, C. A.; Torabi, A.; Nicovich, J. M. *J. Phys. Chem*. **1984**, *88*, 2095.

(6) Margitan, J. J. *J. Phys. Chem*. **1984**, *88*, 3314.

(7) Martin, D.; Jourdain, J. L.; Bras, G. L. *J. Phys. Chem*. **1986**, *90*, 4143.

(8) Lee, Y.-Y.; Kao, W.-C.; Lee, Y.-P. *J. Phys. Chem*. **1990**, *94*, 4535.

(9) Fulle, D.; Hamann, H. F.; Hippler, H.; *Phys. Chem. Chem. Phys.* **1999**, *1*, 2695 and references therein.

(10) Blitz, M. A.; Hughes, K. J.; Pilling, M. J. *J. Phys. Chem*. **2003**, *107*, 1971.

(11) Egsgaard, H.; Carlsen, L.; Florencio, H.; Drewell, T.; Schwarz, H. *Chem. Phys. Lett*. **1988**, *148*, 537.

(12) Hashimoto, S.; Inoue, G.; Akimoto, H. *Chem. Phys. Lett*. **1984**, *107*, 198.

(13) Nagase, S.; Hashimoto, S.; Akimoto, H. *J. Phys. Chem*. **1988**, *92*, 641.

(14) Kuo, Y.-P.; Cheng, B.-M.; Lee., Y.-P. *Chem. Phys. Lett.* **1991**, *177*, 195.

(15) Aaltonen, E. T.; Francisco, J. S. *J. Phys. Chem. A* **2003**, *107*, 1216.

(16) Mielke, Z.; Tokhadze, K. G.; Latajka, Z.; Ratajczak, E. *J. Phys. Chem.* **1996**, *100*, 539.

(17) Mielke, Z.; Latajka, Z.; Kołodziej, J.; Tokhadze, K. G. *J. Phys. Chem*. **1996**, *100*, 11610.

(18) Maillard, D.; Allavena, M.; Perchard, J. P. *Spectrochimica Acta A* **1975**, *31*, 1523.

(19) Nord, L. *J. Mol. Struct*. **1982**, *96*, 19.

(20) Wierzejewska-Hnat, M.; Schriver, A.; Schriver-Mazzuoli, L. *Chem. Phys*. **1994**, *183*, 117.

(21) Schriver-Mazzuoli, L.; Schriver, A.; Wierzejewska-Hnat, M. *Chem. Phys*. **1995**, *199*, 227.

(22) Mielke, Z.; Olbert-Majkut, A.; Tokhadze, K. G. *J. Chem. Phys.* **2003**, *118*, 1364.

(23) Sodeau, J. R.; Lee, E. K. C. *J. Phys. Chem*. **1980**, *84*, 3358.

(24) Wierzejewska, M.; Mielke, Z.; Wieczorek, R.; Latajka, Z. *Chem. Phys*. **1998**, *228*, 17.

(25) Frisch, M. J.; Trucks, G. W.; Schlegel, H. B.; Scuseria, G. E.; Robb, M. A.; Cheeseman, J. R.; Zakrzewski, V. G.; Montgomery, J. A., Jr.; Stratmann, R. E.; Burant, J. C.; Dapprich, S.; Millam, J. M.; Daniels, A. D.; Kudin, K. N.; Strain, M. C.; Farkas, O.; Tomasi, J.; Barone, V.; Cossi, M.; Cammi, R.; Mennucci, B.; Pomelli, C.; Adamo, C.; Clifford, S.; Ochterski, J.; Petersson, G. A.; Ayala, P. Y.; Cui, Q.; Morokuma, K.; Malick, D. K.; Rabuck, A. D.; Raghavachari, K.; Foresman, J. B.; Cioslowski, J.; Ortiz, J. V.; Stefanov, B. B.; Liu, G.; Liashenko, A.; Piskorz, P.; Komaromi, I.; Gomperts, R.; Martin, R. L.; Fox, D. J.; Keith, T.; Al-Laham, M. A.; Peng, C. Y.; Nanayakkara, A.; Gonzalez, C.; Challacombe, M.; Gill, P. M. W.; Johnson, B. G.; Chen, W.; Wong, M. W.; Andres, J. L.; Head-Gordon, M.; Replogle, E. S.; Pople, J. A. *Gaussian 98*, revision A.9; Gaussian, Inc.: Pittsburgh, PA, 1998.

(26) Moller, C.; Plesset, M. S. *Phys. Rev*. **1934**, *46*, 618.

(27) Binkley, J. S.; Pople, J. A. *Int. J. Quantum Chem*. **1975**, *9*, 229.

(28) Müller, R. P.; Nonella, M.; Russegger, P.; Huber J. R. *Chem. Phys.* **1984**, *87*, 351.

(29) Bahou, M.; Lee, Y.-P. *J. Chem. Phys*. **2001**, *115*, 10694.

(30) Hawkins, M.; Downs, A. *J. Phys. Chem*. **1984**, *88*, 3042.

(31) Tchir, P. O.; Spratley, R. D. *Can. J. Chem*. **1975**, *53*, 2318.

(32) Givan, A.; Larsen, L. A.; Loewenschuss, A.; Nielsen, C. J. *J. Mol. Struct*. **1999**, *509*, 35.

(33) Fender, M. A.; Sayed, Y. M.; Prochaska, F. T. *J. Phys. Chem*. **1991**, *95*, 2811.

(34) Smardzewski, R. R.; Lin, M. C. *J. Chem. Phys*. **1977**, *66*, 7.

(35) Kesheng Xu, G. A.; Zhang, J. *J. Phys. Chem. A* **2001**, *105*, 1465.

(36) Hawkins, M.; Downs, A. J. *J. Phys. Chem*. **1984**, *88*, 1527.

(37) Legay, F.; Legay-Sommaire, N. *Chem. Phys. Lett*. **1993**, *211*, 516.

(38) Givan, A.; Loewenschuss, A.; Nielsen, C. J. *Phys. Chem. Chem. Phys.* **1999**, *1*, 37.

(39) Barnes, A. J.; Lasson, E.; Nielsen, C. J. *J. Chem. Soc., Faraday Trans*. **1995**, *91*, 3111.

(40) Davis, S. R.; Andrews, L.; Trindle, C. O. *J. Chem. Phys.* **1987**, *86*, 6027.

(41) Mielke, Z.; Latajka, Z.; Olbert-Majkut, A.; Wieczorek, R. *J. Phys. Chem*. **2000**, *104*, 3764.

(42) De Saxce, A.; Sanna, N.; Schriver, A.; Schriver-Mazzuoli, L. *Chem. Phys*. **1994**, *185*, 365.

(43) Maier, G.; Reisenauer, H. P.; De Marco, M. *Chem. Eur. J*. **2000**, *6*, 800.

(44) Ahlrichs, R.; Schunck, S.; Schnönckel, H. *Angew. Chem., Int. Ed. Engl*. **1988**, *27*, 421.

(45) Cheng, B.-M.; Lee, J.-W.; Lee, Y.-P. *J. Phys. Chem*. **1991**, *95*, 2814.

(46) Maier, G.; Reisenauer, H. P.; Eckwert, J.; Naumann, M.; De Marco, M. *Angew. Chem. Int. Ed. Engl*. **1997**, *36*, 1707.

(47) Jacox, M. E.; Milligan, D. E. *J. Mol. Spectrosc*. **1973**, *48*, 536.

(48) Andrews, L.; Hassanzadeh, P.; Brabson, G. D.; Citra, A.; Neurock, M. *J. Phys. Chem*. **1996**, *100*, 8273.